

Polymer adsorption at liquid/air interfaces under lateral pressure

Vered Aharonson^a, David Andelman^a, Anton Zilman^a,
Philip A. Pincus^b and Elie Raphaël^c

^a*School of Physics and Astronomy, Tel Aviv University, Raymond and Beverly Sackler
Faculty of Exact Sciences, Ramat Aviv, Tel Aviv 69978, Israel*

^b*Materials and Physics Departments, University of California, Santa Barbara, CA 93106,
USA*

^c*Laboratoire de Physique de la Matière Condensée, URA n° 792 du C.N.R.S.,
Collège de France, 75231 Paris Cedex 05, France*

We present calculations of surface tension of adsorbed polymer solutions at the liquid/air interface. Lateral changes in the area per monomer on the surface are induced by changing the surface pressure (lateral compression), while keeping the total surface excess fixed. Lateral compression of the adsorbed layer immersed in a good solvent results in an increase in the surface monomer concentration and surface pressure up to a critical area per monomer value where the compressibility of the system vanishes. Our mean-field model is not appropriate to describe more compressed states. Calculations are repeated in theta and bad solvent conditions, and yield similar behavior of the isotherms.

1. Introduction

Interfacial properties of polymer systems close to solid and liquid surfaces as well as at liquid/liquid interfaces have been investigated in many recent studies [1–10]. Various experiments [11–13] established the existence of an adsorption layer for polymer solutions in the vicinity of an attractive interface, and investigated its dependence on parameters such as monomer concentration, chain length and flexibility, adsorption energy and polymer–solvent interaction. The adsorption layer was interpreted as a self-similar “fluffy carpet” extending up to large distances from the wall in the form of loops and tails [2]. This self-similar structure accounts well for many observed features of adsorbed polymer layers like surface excess and surface tension.

Theoretical studies of polymer solutions at interfaces are based on several different calculational methods. One of the principal approaches used to obtain surface tension in semi-dilute polymer solutions [6] is a modification of the Cahn development [14] for interfacial energies. This treatment, put forward by

de Gennes, gives a qualitative description (on a mean field level) for the interfacial free energy and profiles of the polymer concentration close to the interface. In some related works [3,13] an augmented mean-field theory using scaling arguments (as was applied by Widom for binary liquid mixtures at interfaces [15]) has been extended to polymer solutions. This approach gives more accurate scaling exponents e.g., for the dependence of surface tension on concentration [1].

Surface tension and concentration profiles of polymer solutions at liquid/air interfaces have been studied theoretically and experimentally as a function of solvent quality: good [7], theta [8] and bad [16,17] solvent conditions. The dependence of these surface properties on the polymer bulk concentration has been established and the surface tension of the solution has been measured for different molecular weights and different monomer–interface interaction energies. When the interface–monomer interaction is attractive, an adsorbed polymer layer is formed with a concentration larger than in the bulk. For large (small) values of this interaction, the difference between the surface and bulk concentration of the polymer is also large (small). These two limits have been treated theoretically. As the interface–monomer interaction becomes less and less favorable, at some point, the surface becomes neutral to polymer adsorption. Further reduction of the interface–monomer interaction results in a *depletion* layer created at the interface. Measurements of surface tension of polymer solutions [18] sought this critical attractive-repulsive transition, known as the “special transition”. However, in the following we will consider only the adsorbing (attractive) case.

Polymer adsorption was also considered experimentally and theoretically at solid/liquid interfaces [1,10]. In addition, forces between two polymer layers adsorbed on solid surfaces can be measured and compared to theoretical calculations [9,16,17] as a function of the spacing between the two plates.

We review now the thermodynamics of polymer adsorption on a single flat liquid/air interface (located at $z = 0$). The monomer volume fraction $\Phi(z)$ can then be assumed to depend only on the distance z from interface. The bulk monomer volume fraction is defined as $\Phi_b = \Phi(z \rightarrow \infty)$ and the interfacial free energy γ (per unit area) for semi-dilute polymer solutions (above the chain overlap concentration Φ^*) can be written as

$$\gamma - \gamma_0 = -\gamma_1 \Phi_s + \int_0^\infty dz \left[L(\Phi) \left(\frac{d\Phi}{dz} \right)^2 + F(\Phi) - \mu_b \Phi + \pi_b \right], \quad (1.1)$$

where γ_0 is the surface tension of the pure solvent, $\gamma_1 > 0$ is the local interface–monomer interaction energy per unit area and the volume fraction of the

polymer at the surface is $\Phi_s = \Phi(z = 0)$. The interface interaction term $-\gamma_1 \Phi_s$ is taken negative since we consider an adsorbing interface. The stiffness function $L(\Phi)$ represents the energy cost of making local changes in the polymer concentration [6,7] and for small polymer concentration can be written as

$$L(\Phi) = \frac{k_B T}{a^3} \left(\frac{a^2}{24\Phi} \right), \quad (1.2)$$

where a is the monomer size, k_B the Boltzmann constant and T the temperature. The last three terms in the integral of (1.1) come from the bulk free energy of mixing (per unit volume) $F(\Phi)$, the bulk chemical potential μ_b and the bulk osmotic pressure π_b as defined below,

$$F(\Phi) = \frac{k_B T}{a^3} \left(\frac{\Phi}{N} \log \Phi + \frac{1}{2} v \Phi^2 + \frac{1}{6} w \Phi^3 + \dots \right), \quad (1.3)$$

where N is the degree of polymerization. In the following, we neglect the first term in (1.3) (translational entropy term), as we will take the limit $N \gg 1$. The second and third virial coefficients are v (usually temperature dependent) and w , respectively. For good, theta or bad solvent conditions v is positive, zero or negative, respectively. The chemical potential μ_b and the osmotic pressure π_b are related to the following derivatives of $F(\Phi)$ taken at $\Phi = \Phi_b$:

$$\mu_b = \left(\frac{\partial F}{\partial \Phi} \right)_b, \quad (1.4)$$

$$\pi_b = \left[\Phi^2 \frac{\partial}{\partial \Phi} \left(\frac{F}{\Phi} \right) \right]_b. \quad (1.5)$$

Eqs. (1.1)–(1.5) entirely define the polymer concentration profile $\Phi(z)$ and its surface value Φ_s as function of the bulk concentration Φ_b and the surface interaction parameter γ_1 . In the following we will refer to this state as the equilibrium *reference* state.

The surface excess Γ is defined as the total amount of monomers per unit area which belong to the adsorbing layer,

$$\Gamma = \int_0^{\infty} [\Phi(z) - \Phi_b] dz. \quad (1.6)$$

The *total surface excess* is defined as the product of the total surface area occupied by the layer times Γ .

In this work, we study the effect of a lateral surface compression in analogy to surface pressure–area isotherms of insoluble *Langmuir* monolayers of

surfactant or lipid molecules spread at the liquid/air interface. We apply a surface pressure (which reduces the total surface area occupied by the adsorbing layer) while keeping the total polymer surface excess constant. The justification of keeping this quantity constant is that the system goes through a process of compression by *local* rearrangement of the monomer configurations of the adsorbed layer. For polymer systems, the exchange time scale between the adsorbed layer and the bulk is much longer than the time scale of rearrangement within the layer.

In order to conserve the constraint of fixed total surface excess, we define within the Cahn–de Gennes mean field approach (1.1), a new functional

$$g = \gamma - \gamma_0 + \lambda(k_B T/a^3)\Gamma = -\Pi_s + \lambda(k_B T/a^3)\Gamma, \quad (1.7)$$

where the Lagrange multiplier λ will ensure the conservation of the surface excess, and $\Pi_s = \gamma_0 - \gamma$ is the surface pressure. In agreement with the discussion above, the equilibrium reference state is achieved by setting $\lambda = 0$.

In addition to the surface–monomer interaction, the type of solvent is important in determining the profile and other features of the polymer adsorption layer. We present our results for the good solvent condition in the next section. Theta and bad solvent conditions are considered in sections 3 and 4, respectively. The different solvent conditions are taken into account by choosing the appropriate expression for the bulk free energy $F(\Phi)$. All our calculations are done on a mean-field level in the semi-dilute regime. Concluding remarks follow in section 5.

2. Good solvent

In this section we investigate the response of the system to a lateral pressure of an adsorbed polymer layer in the vicinity of an interface in good solvent conditions. The polymer solution is considered to be in the semi-dilute regime and the interface is an adsorbing one. The free energy density $F(\Phi)$ in good solvent conditions is dominated by the effective two-body repulsion, so one can set in (1.3) $w = 0$, leaving only a positive second virial term, $v > 0$.

2.1. Zero bulk concentration: $\Phi_b = 0$

For clarity, we first considered the limit of vanishing bulk concentration $\Phi_b = \Phi(z = \infty) = 0$. This simplifies considerably the calculations, as the bulk chemical potential (1.4) and osmotic pressure (1.5) in the Cahn–de Gennes functional (1.1) can be set to zero, enabling us to obtain simple expressions for

the system profile and surface tension under compression. A vanishing bulk concentration is compatible with the semi-dilute expression for $F(\Phi)$, as the adsorption layer concentration is always in the semi-dilute range and it is this layer which contributes the most to the interfacial free energy. The more general case of a non-zero bulk concentration follows at the end of this section, where some of the integrations are carried out numerically.

Substituting $\Phi_b = 0$ in (1.1)–(1.7) while remembering that in this case μ_b and π_b are also zero, we obtain for the functional g ,

$$g = -\gamma_1 \Psi_s^2 + \frac{k_B T}{a^3} \int_0^\infty dz \left[\frac{1}{6} a^2 \left(\frac{d\Psi}{dz} \right)^2 + \frac{1}{2} v \Psi^4 + \lambda \Psi^2 \right], \quad (2.1)$$

where $\Psi = \sqrt{\Phi}$ is defined as a convenient order parameter. In a dimensionless form, the functional $\tilde{g} \equiv g/\gamma_1$ is

$$\tilde{g} = -\Psi_s^2 + \sigma^{-1} \int_0^\infty d\eta \left[\left(\frac{d\Psi}{d\eta} \right)^2 + \Psi^4 + \tilde{\lambda} \Psi^2 \right], \quad (2.2)$$

where the distance from the surface z was normalized by the correlation length $\xi = a/\sqrt{3v}$ and the new dimensionless integration variable is $\eta \equiv z/\xi$. The constant $\sigma^{-1} \equiv k_B T/6\gamma_1 a \xi$ is the dimensionless adsorption coefficient and $\tilde{\lambda} \equiv 2\lambda/v$. The functional minimization of \tilde{g} with respect to $\Psi(\eta)$ gives the Euler–Lagrange equation

$$\frac{d^2 \Psi}{d\eta^2} = 2\Psi^3 + \tilde{\lambda} \Psi. \quad (2.3)$$

A first integration of (2.3) yields

$$\frac{d\Psi}{d\eta} = -\sqrt{\Psi^4 + \tilde{\lambda} \Psi^2}, \quad (2.4)$$

while a second integration gives the polymer concentration profile $\Phi(\eta) = \Psi^2(\eta)$,

$$\Psi(\eta) = \frac{\sqrt{\tilde{\lambda}}}{\sinh[\sqrt{\tilde{\lambda}} \eta + \sinh^{-1}(\sqrt{\tilde{\lambda}}/\Psi_s)]}. \quad (2.5)$$

Further minimization of the functional (2.2) with respect to Ψ_s gives a relation between the Lagrange coefficient $\tilde{\lambda}$ and the monomer surface fraction $\Phi_s = \Psi_s^2$,

$$\tilde{\lambda} = \sigma^2 - \Psi_s^2 = \sigma^2 - \Phi_s. \quad (2.6)$$

Inserting this relation into the constraint (1.6) yields the expression of Φ_s and $\tilde{\lambda}$ in terms of the rescaled (dimensionless) area per monomer \mathcal{A} :

$$\mathcal{A}^{-1} \equiv \Gamma/\xi, \quad (2.7)$$

$$\tilde{\lambda}/\sigma^2 = (1 - \sigma^{-1}\mathcal{A}^{-1})^2, \quad (2.8)$$

$$\Phi_s/\sigma^2 = 1 - (1 - \sigma^{-1}\mathcal{A}^{-1})^2 = 1 - \tilde{\lambda}/\sigma^2. \quad (2.9)$$

Note that although the Lagrange multiplier enters into the functional g , the surface pressure Π_s , even in presence of the constraint (1.6), is always equal to $\gamma_0 - \gamma$, eq. (1.7). Inserting (2.4) into (2.2), while substituting $\tilde{\lambda}$ from (2.8), the surface pressure can be evaluated analytically as an integral over Ψ ,

$$\begin{aligned} \tilde{\Pi}_s &\equiv \frac{\Pi_s}{\gamma_1} = \Psi_s^2 - \sigma^{-1} \int_0^{\Psi_s} d\Psi [2\Psi(\Psi^2 + \tilde{\lambda})^{1/2} - \tilde{\lambda}\Psi(\Psi^2 + \tilde{\lambda})^{-1/2}] \\ &= \frac{\sigma^2}{3} \left(\frac{1}{(\sigma\mathcal{A})^3} - \frac{3}{(\sigma\mathcal{A})^2} + \frac{3}{\sigma\mathcal{A}} \right). \end{aligned} \quad (2.10)$$

The dependence of Φ_s , $\tilde{\lambda}$ and $\tilde{\Pi}_s$ on \mathcal{A} are plotted in fig. 1.

The region of $\mathcal{A} > \sigma^{-1}$ in fig. 1 corresponds to an experiment where the surface undergoes an *expansion* beyond its equilibrium reference state, $\mathcal{A} = \sigma^{-1}$, and its isotherm is given by eq. (2.10). When \mathcal{A} is large, the Lagrange multiplier $\tilde{\lambda}$ is constant, equals to σ^2 , eq. (2.8), and decreases with diminishing surface area, while the surface pressure (2.10) varies as $1/\mathcal{A}$ similar to an ideal gas isotherm. As \mathcal{A} decreases, deviations from an ideal gas behavior are noticed. Moreover, as the equilibrium reference state $\mathcal{A} = \sigma^{-1}$ is reached, the Lagrange multiplier vanishes and the surface fraction Φ_s has a maximum. Concurrently, the surface pressure saturates at a maximum value with vanishing slope, leading to a zero compressibility.

Below the equilibrium reference state, the solution of eq. (2.9) ceases to be physical as $\Psi_s^2 < 0$. Therefore, compression of the film (good solvent condition and $\Phi_b = 0$) beyond the reference state cannot be described by our model.

2.2. Nonzero bulk concentration: $\Phi_b > 0$

The above considered case ($\Phi_b = 0$ together with the constraint of fixed total surface excess) may be too limiting. Therefore, we have also studied the more

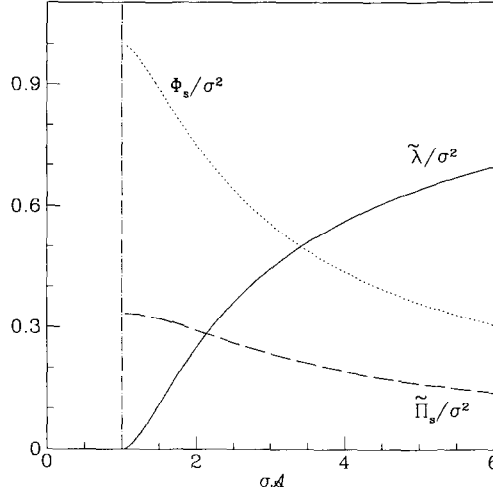


Fig. 1. The surface concentration Φ_s/σ^2 , Lagrange multiplier $\tilde{\lambda}/\sigma^2$ and surface pressure $\tilde{\Pi}_s/\sigma^2$ are shown as function of the rescaled area per monomer $\sigma\mathcal{A}$. See also eqs. (2.7)–(2.10). The solvent is good and the bulk concentration Φ_b is set to zero.

general case of finite bulk concentration Φ_b (keeping the constraint of fixed surface excess). The functional \tilde{g} , with a normalized order parameter $y^2 \equiv \Phi(z)/\Phi_b$, can then be calculated from (1.1). One obtains

$$\frac{\tilde{g}}{\Phi_b} = -y_s^2 + \sigma^{-1} \int_0^\infty d\eta \left[\left(\frac{dy}{d\eta} \right)^2 + (y^2 - 1)^2 + \tilde{\lambda}(y^2 - 1) \right], \quad (2.11)$$

where the correlation length ξ depends now on Φ_b , $\xi \equiv a/\sqrt{3v\Phi_b}$, $\eta \equiv z/\xi$ is the dimensionless integration variable, $\sigma^{-1} = k_B T/6\gamma_1 a \xi$ is the dimensionless adsorption coefficient and $\tilde{\lambda} \equiv 2\lambda/v\Phi_b$.

It is now straightforward to obtain the integral forms of the other quantities: Π_s and $\mathcal{A} = \xi/\Gamma$ from eq. (2.7). By repeating the same procedure of taking the functional derivative with respect to the polymer profile and its surface value (as in the $\Phi_b = 0$ case) we obtain

$$\frac{\tilde{g}}{\Phi_b} = \frac{g}{\gamma_1 \Phi_b} = -y_s^2 + 2\sigma^{-1} \int_1^{y_s} dy \sqrt{(y^2 - 1)(y^2 - 1 + \tilde{\lambda})}, \quad (2.12)$$

$$\frac{\tilde{\Pi}_s}{\Phi_b} = \frac{\Pi_s}{\gamma_1 \Phi_b} = -\frac{\tilde{g}}{\Phi_b} + (\mathcal{A}\Phi_b)^{-1} \sigma^{-1} \tilde{\lambda}, \quad (2.13)$$

$$(\mathcal{A}\Phi_b)^{-1} = \int_1^{y_s} dy \sqrt{\frac{y^2 - 1}{y^2 - 1 + \tilde{\lambda}}}, \quad (2.14)$$

and from the boundary condition

$$\tilde{\lambda} = \frac{\sigma^2 y_s^2}{y_s^2 - 1} - (y_s^2 - 1). \quad (2.15)$$

Because of the complexity of the integrals involved, $\tilde{\Pi}_s(\mathcal{A})$ and $y_s(\mathcal{A})$ are evaluated numerically in the following way. First $\mathcal{A}(y_s)$ and $\lambda(y_s)$ are evaluated from (2.14) and (2.15), respectively for a given value of σ – the only remaining free parameter. Then, those functions are substituted in (2.12) and (2.13) in order to obtain $\Phi_s(\mathcal{A})$ and the isotherm $\Pi_s(\mathcal{A})$ can be seen in figs. 2 and 3, respectively. The isotherm shown in fig. 3 is quite similar to the one for zero bulk concentration (fig. 1) as the pressure saturates (with zero slope) at the equilibrium reference state ($\tilde{\lambda}=0$). No further compression is allowed within our model below this point. Note that the limit of zero Φ_b can be obtained formally from eqs. (2.12)–(2.15) by looking at the limit of $\sigma \rightarrow \infty$ of properly rescaled variables.

Hence, a non-zero bulk concentration does not change the main features of the process of lateral compression discussed above. In particular, the compres-

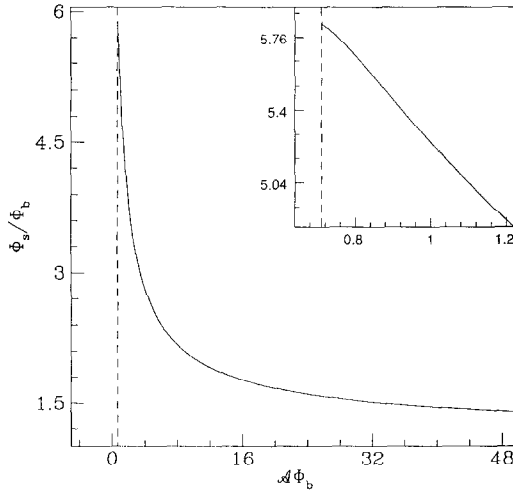


Fig. 2. Surface value of Φ , normalized as $\Phi_s/\Phi_b = y_s^2$ vs. rescaled area per monomer $\mathcal{A}\Phi_b$ for nonzero Φ_b , good solvent conditions and $\sigma = 2$. The inset shows the region close to the equilibrium reference state ($\tilde{\lambda}=0$), beyond which there is no solution to our isotherm equation. See eqs. (2.12)–(2.15).

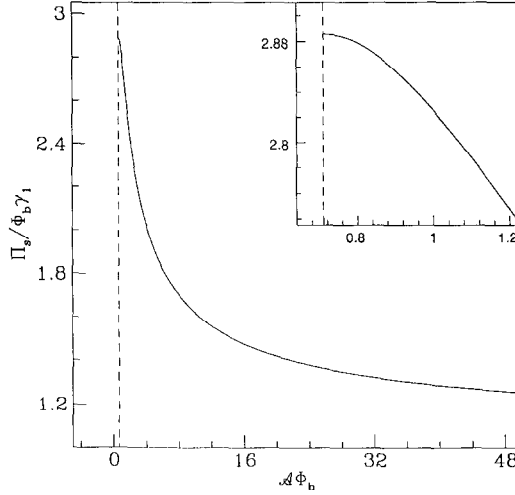


Fig. 3. Surface pressure, normalized as $\tilde{\Pi}_s/\Phi_b = \Pi_s/\Phi_b\gamma_1$ vs. rescaled area per monomer $\mathcal{A}\Phi_b$ for nonzero Φ_b , good solvent conditions and $\sigma = 2$. The inset shows the region close to the plateau (equilibrium reference state) beyond which there is no solution to our isotherm equation. See eqs. (2.12)–(2.15).

sion below the reference state cannot be described by our model. Physically, it is quite likely that below the equilibrium reference state, the polymers in the adsorbed layer are extended in a manner somewhat similar to “polymer brushes” (grafted polymers) [19] or “pseudo-brushes” (irreversible adsorption) [20] with many anchoring sites. However, such extended states are beyond our simple mean-field approach.

3. Theta solvent

We now turn to the case of theta solvent conditions following the general formalism of section 1. A positive w term in (1.3) is used, because the monomer–monomer repulsion vanishes ($v = 0$) in theta conditions, yielding a different calculation than for the good solvent case ($v > 0$).

3.1. Zero bulk concentration: $\Phi_b = 0$

In the case of $\Phi_b = 0$, the bulk chemical potential (1.4) and osmotic pressure (1.5) are both zero and the functional \tilde{g} , defined in the last section, is simply

$$\tilde{g} \equiv \frac{\mathcal{G}}{\gamma_1} = -\Psi_s^2 + \sigma^{-1} \int_0^\infty d\eta \left[\left(\frac{d\Psi}{d\eta} \right)^2 + \Psi^6 + \tilde{\lambda}\Psi^2 \right], \quad (3.1)$$

where $\Psi = \sqrt{\Phi}$ is the order parameter, $\xi = a/\sqrt{w}$ is the appropriate correlation length, and $\eta \equiv z/\xi$. The dimensionless Lagrange coefficient here is $\tilde{\lambda} = 6\lambda/w$ and $\sigma^{-1} \equiv k_B T/6\gamma_1 a\xi$ is the dimensionless adsorption coefficient.

Minimization with respect to Ψ gives the profile equations

$$\frac{d^2\Psi}{d\eta^2} = 3\Psi^5 + \tilde{\lambda}\Psi. \quad (3.2)$$

Integrating the above equation twice yields the polymer profile $\Phi(\eta)$,

$$\Phi(\eta) = \frac{\sqrt{\tilde{\lambda}}}{\sinh[2\sqrt{\tilde{\lambda}}\eta + \sinh^{-1}(\sqrt{\tilde{\lambda}}/\Phi_s)]}. \quad (3.3)$$

The other relations take the following forms:

$$\Phi_s = \sigma \tanh(2\mathcal{A}^{-1}), \quad (3.4)$$

$$\tilde{\lambda} = \sigma^2 - \Phi_s^2 = \sigma^2 [\cosh(2\mathcal{A}^{-1})]^{-2} \quad (3.5)$$

and

$$\tilde{\Pi}_s = \frac{1}{2}\sigma \tanh(2\mathcal{A}^{-1}), \quad (3.6)$$

where \mathcal{A} is defined by eq. (2.7) with $\xi = a/\sqrt{w}$. These relations are plotted in fig. 4.

From eq. (3.6) and fig. 4 it is apparent that the pressure reaches a ‘‘plateau’’ at zero area per monomer. This should be compared with the good solvent case, where a similar plateau is reached for a finite value of \mathcal{A} (the equilibrium reference state). The reason of this plateau at zero \mathcal{A} is the following. For the theta solvent, the equilibrium reference state ($\tilde{\lambda} = 0$) occurs exactly at $\mathcal{A} = 0$ since the integrated surface excess Γ has a logarithmic divergence (as long as $\Phi_b = 0$) as can be seen from eq. (3.3). Hence, a compression of the monolayer is possible till $\mathcal{A} = 0$ (the equilibrium reference state).

3.2. Nonzero bulk concentration: $\Phi_b > 0$

Repeating the previous analysis for non-zero bulk polymer concentration $\Phi_b > 0$, we obtain for the surface free energy

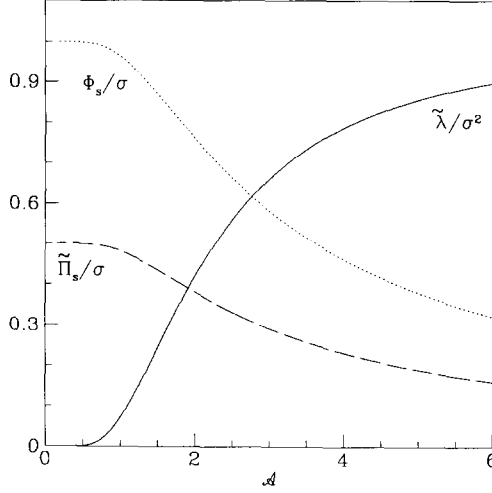


Fig. 4. The surface concentration Φ_s/σ , Lagrange multiplier $\tilde{\lambda}/\sigma^2$ and surface pressure $\tilde{\Pi}_s/\sigma$ are shown as function of the rescaled area per monomer \mathcal{A} . The calculation is done for a theta solvent using eqs. (3.4)–(3.6) for zero bulk concentration ($\Phi_b = 0$).

$$\begin{aligned} \frac{\tilde{g}}{\Phi_b} &= \frac{g}{\gamma_1 \Phi_b} \\ &= -y_s^2 + \sigma^{-1} \int_0^{\infty} d\eta \left[\left(\frac{dy}{d\eta} \right)^2 + (y^2 + 2)(y^2 - 1)^2 + \tilde{\lambda}(y^2 - 1) \right], \end{aligned} \quad (3.7)$$

where y and y_s are the dimensionless order parameters defined in the previous section, the correlation length and Lagrange multiplier are $\xi = a/\sqrt{w}\Phi_b$ and $\tilde{\lambda} \equiv 6\lambda/w\Phi_b^2$, respectively, and $\sigma^{-1} = k_B T/6\gamma_1 a\xi$.

As in the good solvent case, the isotherm and related quantities can be obtained from the following expressions:

$$\frac{\tilde{g}}{\Phi_b} = -y_s^2 + 2\sigma^{-1} \int_1^{y_s} dy \sqrt{(y^2 - 1)(y^4 + y^2 - 2 + \tilde{\lambda})}, \quad (3.8)$$

$$\frac{\tilde{\Pi}_s}{\Phi_b} = \frac{\Pi_s}{\gamma_1 \Phi_b} = -\frac{\tilde{g}}{\Phi_b} + \sigma^{-1} (\mathcal{A}\Phi_b)^{-1} \tilde{\lambda}, \quad (3.9)$$

$$(\mathcal{A}\Phi_b)^{-1} = \int_1^{y_s} dy \sqrt{\frac{y^2 - 1}{y^4 + y^2 - 2 + \tilde{\lambda}}} \quad (3.10)$$

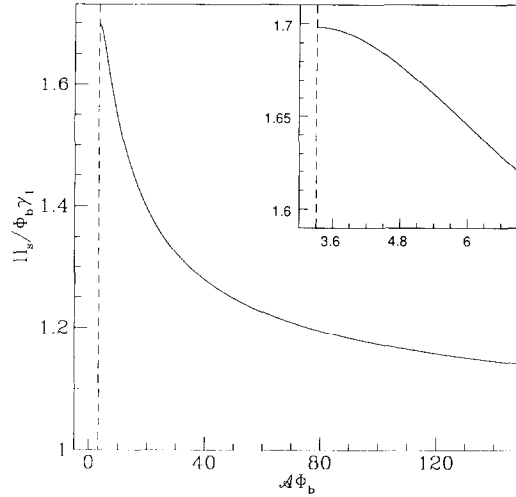


Fig. 5. Surface pressure, normalized as $\Pi_s / \Phi_b \gamma_1$, vs. area per monomer $\mathcal{A} \Phi_b$ for theta solvent conditions with a general value of Φ_b and $\sigma = 2$. The inset shows the plateau region close to the equilibrium reference state ($\tilde{\lambda} = 0$) beyond which there is no solution to our isotherm equation. See eqs. (3.8)–(3.11).

and

$$\tilde{\lambda} = \frac{\sigma^2 y_s^2}{y_s^2 - 1} - (y_s^4 + y_s^2 - 2). \quad (3.11)$$

A numerical calculation of the surface pressure as a function of area per monomer is shown in fig. 5. Unlike the case of theta solvent with zero bulk value, here the plateau in the isotherm is reached for a finite value of \mathcal{A} . However, as in the good solvent case, the limit of zero Φ_b can be obtained from eqs. (3.8)–(3.11) by looking at the $\sigma \rightarrow \infty$ limit.

4. Bad solvent

The most obvious feature for bad solvents is that the bulk free energy is bi-stable, as the system is composed of two coexisting phases: one rich in polymer and another one which is poor in polymer. In bad solvent conditions, the bulk free energy density expansion $F(\Phi)$ in (1.3) contains a negative second virial coefficient $v = \alpha(T - T_c) < 0$ which is stabilized by a positive third virial coefficient $w > 0$.

The phase diagram, fig. 6, presents the coexistence curve $v(\Phi)$ which separates the single phase region from the two-phase one. The two branches of

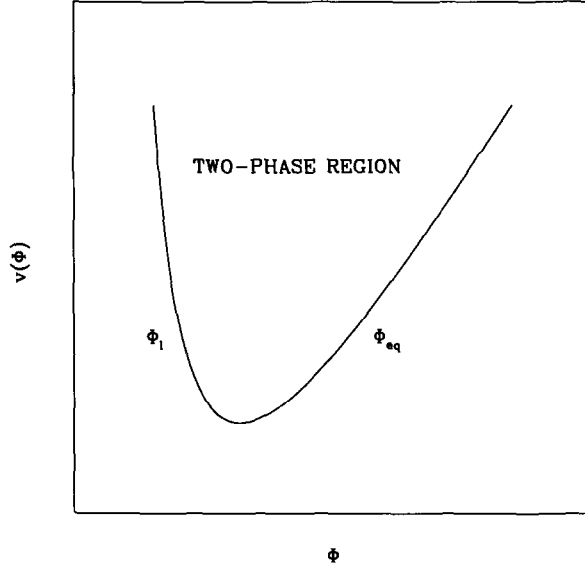


Fig. 6. Flory-Huggins phase diagram for a polymer-bad-solvent mixture, where v is the second virial coefficient and Φ is the polymer volume fraction. The coexistence curve $v(\Phi)$ separates the one-phase from the two-phase region. The values of the volume fraction on the dilute and semi-dilute branches of the coexistence curve are Φ_l and Φ_{eq} , respectively.

the coexistence curve are the very dilute branch, Φ_l , where the osmotic pressure can be set approximately to zero, and the semi-dilute one, Φ_{eq} . The semi-dilute volume fraction Φ_{eq} can be estimated by equating the osmotic pressures and chemical potentials in the two coexisting phases [10,16,17] yielding

$$\Phi_{eq} \approx \frac{3|v|}{2w} \tag{4.1}$$

and

$$\pi_{eq} \approx 0, \quad \mu_{eq} \approx -\frac{3k_B T}{8a^3} \left(\frac{v^2}{w}\right). \tag{4.2}$$

For $\Phi_b > \Phi_l$, the free energy functional $\tilde{g} = g/\gamma_1$ is given by

$$\frac{\tilde{g}}{\hat{\Phi}} = -y_s^2 + \sigma^{-1} \int_0^\infty d\eta \left[\left(\frac{dy}{d\eta}\right)^2 + (y^2 - 1)^2 y^2 + \tilde{\lambda}(y^2 - 1) \right], \tag{4.3}$$

where $\eta = z/\xi$ with $\xi = a(3/2v\hat{\Phi})^{1/2}$, and $y \equiv \sqrt{\Phi/\hat{\Phi}}$. For $\Phi_b > \Phi_{eq}$, there is no

phase separation and $\hat{\Phi}$ is equal to the bulk value, Φ_b . On the other hand, for $\Phi_e < \Phi_b < \Phi_{cq}$, the coexistence of two different phases in the bulk (fig. 6) introduces a second interface in the system. For an adsorbing liquid/air interface, one may consider here that the more concentrated phase lies closer to the interface. If this phase can be considered as macroscopically thick, we can set $\hat{\Phi} = \Phi_{cq}$, assuming the second, more dilute, phase to have no influence.

The isotherm of surface pressure vs. area presented in fig. 7 is very similar to the one for the theta solvent case. It is obtained from numerically solving the following equations:

$$\frac{\tilde{g}}{\hat{\Phi}} = -y_s^2 + 2\sigma^{-1} \int_1^{y_s} dy \sqrt{(y^2 - 1)(y^4 - y^2 + \tilde{\lambda})}, \quad (4.4)$$

$$\frac{\tilde{\Pi}_s}{\hat{\Phi}} = \frac{\Pi_s}{\gamma_1 \hat{\Phi}} = -\frac{\tilde{g}}{\hat{\Phi}} + \sigma^{-1} (\mathcal{A}\hat{\Phi})^{-1} \tilde{\lambda}, \quad (4.5)$$

$$(\mathcal{A}\hat{\Phi})^{-1} = \int_1^{y_s} dy \sqrt{\frac{y^2 - 1}{y^4 - y^2 + \tilde{\lambda}}} \quad (4.6)$$

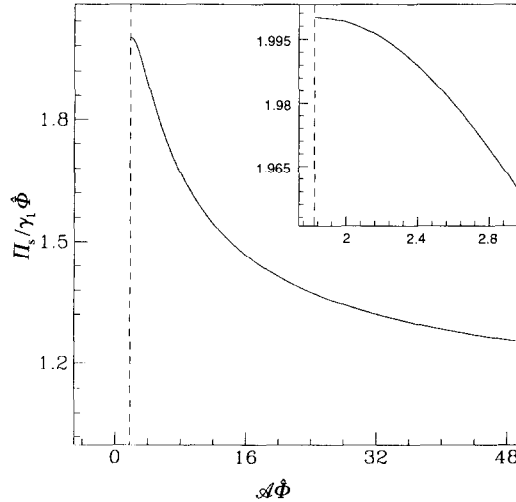


Fig. 7. Same as fig. 5 but with $F(\Phi)$ chosen for bad solvent conditions where $\hat{\Phi}$ is replacing the bulk value Φ_b and $\sigma = 2$. See eqs. (4.3)–(4.7).

and

$$\tilde{\lambda} = \frac{\sigma^2 y_s^2}{y_s^2 - 1} - (y_s^4 - y_s^2). \quad (4.7)$$

A more complicated case arises when the bulk concentration is dilute, $\Phi_b < \Phi_\ell$. In this case the concentration in the vicinity of the liquid/air interface passes through an unstable region. This problem was previously discussed [16,17] and is beyond the scope of the present work.

5. Concluding remarks

In this work we have investigated surface pressure of polymer solutions at a liquid/air interface under lateral compression. We have presented mean field calculations based on the Cahn–de Gennes formalism [6,14]. The important qualitative feature of this work is seen in the isotherms: surface pressure plotted vs area at constant temperature.

The system is found to be characterized by two parameters. One is the strength of the attractive polymer–interface interaction energy γ_1 , measuring the degree of adsorption. The other is the bulk volume fraction Φ_b , which can take different values, according to the preparation of the solution. It is the ratio of these two parameters that appears in the dimensionless adsorption coefficient $\sigma^{-1} = T/6a\gamma_1\xi \sim (T/a^2\gamma_1)\Phi_b^\beta$, where $\beta = 1/2$ for good solvent conditions and $\beta = 1$ for the theta case. A large γ_1 or a small Φ_b corresponds to a large adsorption coefficient.

In all solvent conditions our model does not allow compression beyond the equilibrium reference state for which the system compressibility is zero. Mean field calculation does not provide an insight in the nature of the possible compressed adsorbed polymer layer (beyond the equilibrium reference state). It may be interesting to use other theoretical methods, such as scaling arguments in order to understand better all the possible states of the adsorbed polymer layer. Another extension of our work can be to study the properties of adsorbed polymers on heterogeneous surfaces such as surfactant monolayers [21–23] under lateral compression.

Experiments to verify our finding can be carried out using a Langmuir trough where a horizontal float applies lateral pressure on the polymer adsorbed layer. The polymer solution can then be washed off, fixing the bulk concentration to zero, thus preventing the adsorbed polymers from moving to the other side of the float. Another method is to add a surfactant to the area swept by the float, thus creating an asymmetry in the surface area (one part of it being occupied

by polymers only, while the other by surfactants and polymers). Yet, another possibility is to use a conic trough instead of a float [24]. As the solution is pumped out of the trough, the surface area decreases and no exchange of polymers with the bulk takes place. It will be interesting to verify some of our findings using such experimental set ups and possibly others.

Acknowledgements

We would like to thank P.G. de Gennes for introducing us to this problem and for his on-going interest. We also benefited from discussions with L. Auvray, R. Cantor, D. Chatenay, J.M. di Meglio, O. Guiselin, J.F. Joanny, S. Safran, U. Steiner, I. Szleifer and B. Widom. We would like to acknowledge partial support from the Israel Academy of Sciences and Humanities, the German-Israel Binational Foundation (GIF) under grant No. I-0197 and the U.S. Department of Energy under grant No. DE-FG03-87ER45288.

References

- [1] J.F. Joanny, L. Leibler and P.-G. De Gennes, *J. Polymer. Sci.* 17 (1979) 1073.
- [2] P.-G. De Gennes, *Adv. Colloid Interface Sci.* 27 (1987) 189.
- [3] P.-G. De Gennes and P. Pincus, *J. Phys. Lett. (Paris)* 44 (1983) 241; 45 (1984) 953.
- [4] G. Fleer and J.M.H.M. Scheutjens, *Adv. Colloid Interface Sci.* 16 (1982) 341; *Macromolecules* 18 (1985) 1882.
- [5] G. Rossi and P. Pincus, *Europhys. Lett.* 5 (1988) 641.
- [6] P.-G. De Gennes, *Macromolecules* 14 (1981) 1637.
- [7] R. Ober, L. Paz, C. Taupin and P. Pincus, *Macromolecules* 16 (1983) 50.
- [8] J.M. Di Meglio, R. Ober, L. Paz, C. Taupin and P. Pincus, *J. Phys. (Paris)* 44 (1983) 1035.
- [9] P.-G. De Gennes, *Macromolecules* 15 (1982) 492.
- [10] J. Klein and P. Pincus, *Macromolecules* 15 (1982) 1129.
- [11] M. Cohen Stuart, T. Cosgrove and B. Vincent, *Adv. Colloid Interface Sci.* 24 (1986) 143.
- [12] L. Auvray and J.P. Cotton, *Macromolecules* 20 (1987) 202.
- [13] M. Cohen Stuart, Ph.D. Thesis, Wageningen University (1980), unpublished.
- [14] J.W. Cahn and J.E. Hilliard, *J. Chem. Phys.* 28 (1958) 258.
- [15] B. Widom, in: *Phase Transitions and Critical Phenomena*, vol. 2, C. Domb and M. Green, eds. (Academic Press, New York, 1972).
- [16] K. Ingersent, J. Klein and P. Pincus, *Macromolecules* 19 (1986) 1374.
- [17] K. Ingersent, J. Klein and P. Pincus, *Macromolecules* 23 (1990) 548.
- [18] J.M. Di Meglio and C. Taupin, *Macromolecules* 22 (1988) 2388.
- [19] S. Milner, *Science* 251 (1991) 905.
- [20] O. Guiselin, *Europhys. Lett.* 17 (1992) 225.
- [21] T. Odjik, *Macromolecules* 23 (1990) 1875.
- [22] P.-G. De Gennes, *J. Phys. Chem.* 94 (1990) 8407.
- [23] D. Andelman and J.F. Joanny, *J. Phys. II (France)* 3 (1993) 121.
- [24] B.M. Abrahams, K. Miyano, S.Q. Xu and J.B. Ketterson, *Rev. Sci. Instrum.* 54 (1983) 121.



Erratum

Erratum to “Polymer adsorption at liquid/air interfaces under lateral pressure”
[Physica A 204 (1994) 1–16] ★

Vered Aharonson^a, David Andelman^a, Anton Zilman^a,
Philip A. Pincus^b, Elie Raphaël^c

^a School of Physics and Astronomy, Tel Aviv University, Raymond and Beverly Sackler Faculty of Exact Sciences, Ramat Aviv, Tel Aviv 69978, Israel

^b Materials and Physics Departments, University of California, Santa Barbara, CA 93106, USA

^c Laboratoire de Physique de la Matière Condensée, URA no. 792 du C.N.R.S., Collège de France, 75231 Paris Cedex 05, France

In a paper we have recently published [1], we looked at polymer adsorption at liquid/air interfaces under lateral pressure. However, the calculations of the surface pressure–area isotherms presented in [1] are not correct and should be modified as follows. The surface pressure is always equal to the difference between γ_0 and γ , i.e., $\Pi_s = -(\gamma - \gamma_0)$, where γ and γ_0 are the surface tension and the bare surface tension, respectively. However, $\gamma - \gamma_0$ is given by the right hand side of Eq. (1.1) only at true equilibrium (defined in [1] as the *equilibrium reference state*). In the presence of a fixed *total surface excess* (as defined in [1] after Eq. (1.6)), the difference in surface tensions, $\gamma - \gamma_0$, is equal to the functional g defined correctly in the paper as

$$g = -\gamma_1 \Phi_s + \int_0^\infty dz \left[L(\Phi) \left(\frac{d\Phi}{dz} \right)^2 + F(\Phi) - \mu_b \Phi + \pi_b \right] + \lambda (k_B T / a^3) \Gamma. \quad (1)$$

The surface pressure Π_s can, therefore, be obtained simply from the relation

$$\Pi_s = -g.$$

Although in [1] we correctly calculated the thermodynamics from g as is defined above, the expression associated with the pressure Π_s did not include the last term (proportional to λ) of g in Eq. (1). This means the following changes for the surface pressure:

★ SSDI of original article: 0378-4371(93)E0394-T.

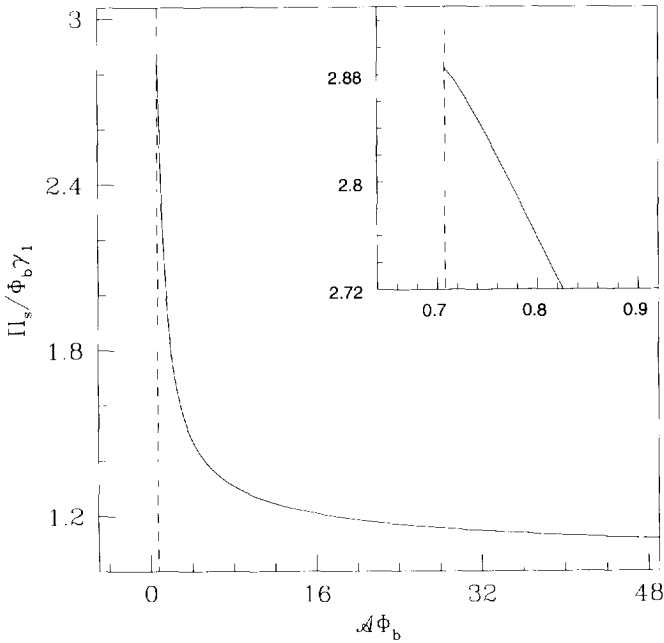


Fig. 1. Surface pressure, normalized as $\tilde{\Pi}_s/\Phi_b = \Pi_s/\Phi_b\gamma_1$ vs rescaled area per monomer $\mathcal{A}\Phi_b$ for nonzero Φ_b , good solvent conditions and $\sigma = 2$. The inset shows the region close to the plateau (equilibrium reference state) beyond which there is no solution to our isotherm equation.

- *Good solvent, $\Phi_b = 0$* : Eq. (2.10) should be replaced by

$$\tilde{\Pi}_s = \frac{\Pi_s}{\gamma_1} = \frac{1}{3}\sigma^2 \left(\frac{3}{(\sigma\mathcal{A})^2} - \frac{2}{(\sigma\mathcal{A})^3} \right). \tag{2}$$

Note that the variation of the surface pressure at large \mathcal{A} does not follow the ideal gas law ($\sim 1/\mathcal{A}$). This can be understood since all entropic terms related to translational entropy of the chains have been neglected in Eq. (1.3). One can check that the derivative of Π_s with respect to \mathcal{A} is indeed zero at the equilibrium reference state $\sigma\mathcal{A} = 1$.

- *Good solvent, non-zero bulk concentration, $\Phi_b > 0$* : $\tilde{\Pi}_s$ calculated numerically in [1] from Eq. (2.13) and plotted there in Fig. 3, should be replaced by $-\tilde{g}$ as is correctly defined in Eq. (2.11). Numerical calculations are presented here in Fig. 1.
- *Theta solvent, zero bulk concentration, $\Phi_b = 0$* : Using $\tilde{\Pi}_s = -\tilde{g}$ we get the following analytical expression for the pressure:

$$\tilde{\Pi}_s = \frac{1}{2}\sigma \tanh(2\mathcal{A}^{-1}) - \frac{\sigma}{\mathcal{A}} [\cosh(2\mathcal{A}^{-1})]^{-2}. \tag{3}$$

This analytical expression should be replotted instead of the one appeared on the original Fig. 4.

- *Theta solvent, non-zero bulk concentration, $\Phi_b > 0$* : The numerical calculation of the pressure in Eq. (3.9) was redone with the correct definition of $\tilde{\Pi}_s = -\tilde{g}$, where \tilde{g} is

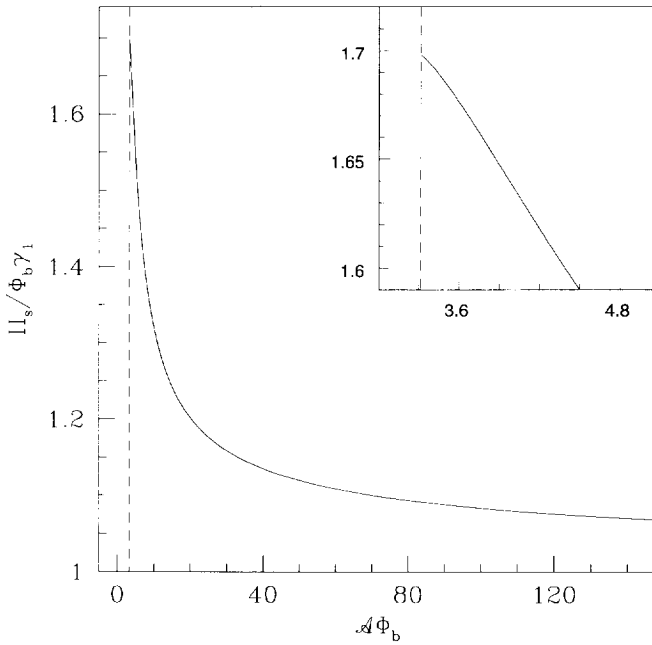


Fig. 2. Surface pressure, normalized as $\Pi_s/\Phi_b\gamma_1$, vs area per monomer $\mathcal{A}\Phi_b$ for theta solvent conditions with a general value of Φ_b and $\sigma = 2$. The inset shows the plateau region close to the equilibrium reference state ($\tilde{\lambda} = 0$) beyond which there is no solution to our isotherm equation.

given by the original Eq. (3.7). The isotherm based on this numerical calculation is presented here in Fig. 2 and should replace the original Fig. 5 in [1].

– *Bad solvent*: The pressure is calculated from \tilde{g} of Eq. (4.4) and not via Eq. (4.5).

We would like to remark that beside these corrections in the calculation of the surface pressure, the other equations for the profile $\Phi(z)$, the surface volume fraction of the polymer at the surface Φ_s , and the Lagrange multiplier λ remain correct.

References

- [1] V. Aharonson, D. Andelman, A. Zilman, P. A. Pincus and E. Raphael, Physica A 204 (1994) 1–16.